

# Econoquantumphysics and econonetwork: do correlations and eigenstates shape the taxonomy of the cryptocurrency market?

C. R. da Cunha, R. da Silva

Instituto de Física, Universidade Federal do Rio Grande do Sul, 91501-970 Porto Alegre, Rio Grande do Sul, Brazil

E-mail: creq@if.ufrgs.br

**Abstract.** We investigate 17 digital currencies making an analogy with quantum systems and develop the concept of eigenportfolios. We show that the density of states of the correlation matrix of these assets shows a behavior between that of the Wishart ensemble and one whose elements are Cauchy distributed. A metric for the participation matrix based on superposition of Gaussian functions is proposed and we show that small eigenvalues correspond to localized states. Nonetheless, some level of localization is also present for bigger eigenvalues probably caused by the fat tails of the distribution of returns of these assets. We also show through a clustering study that the digital currencies tend to stagger together. We conclude the paper showing that this correlation structure leads to an Epps effect.

*Keywords:* bitcoin, quantum, econophysics

## 1. Introduction

Digital currencies are financial assets deprived of an issuing agent constructed on a peer-to-peer managed distributed ledger platform called blockchain. Consensus about the trading of these assets is decentralized, thus they resemble physical autonomous agents that operate out of equilibrium but often reach some steady state regimes where financial returns are characterized by some power law [1]. For instance, bitcoin [2], the most popular digital currency has attracted the attention of the scientific community despite of any criticism that one might have about its use. For example, it has been shown that bitcoin shows the same persistence of spin systems and exhibits crises that resemble naturally occurring earthquakes [3].

Since the development of bitcoin in 2008, many other digital coins appeared in the market as a result of successive forks of its main code. This has happened mainly as a tendency for differentiation in order to make the asset more suitable for specific purposes in a clear case of Darwinian adaptation [4]. There are over 4000 different digital coins available today but only a few have a significant market cap and attract the attention of investors.

In this paper we have a bold proposal: investigate the structure of the market of cryptocurrencies and seek analogies with some aspects of physical quantum systems. We particularly think that portfolios of such currencies resemble quantum mechanical systems and we believe that properties of localization of their eigenmodes suggest a strong and interesting connection between stock markets and quantum mechanics. Similar connections between physical and economic systems have been defining the field of Econophysics [5].

Furthermore, we show that these coins have a natural tendency of clustering that we investigate studying the minimum spanning tree formed by connecting these assets according to their spectral properties. Finally, we show that the asynchronicity in the trading orders of these coins may produce the well known Epps effect.

We divide the paper as follows. In section 2 we present the data used in this paper as well as some fundamental background connecting random matrices, crypto markets, and correlations. We also describe the notation to be used along the paper. In the following section (section 3) we present a brief theoretical formulation and our main results context separated in a few subsections. Finally our summaries and conclusions are briefly explained in section 4.

## 2. Data, Random Matrices, Crypto Markets, and Correlations

The historical series for  $M = 20$  digital assets were directly downloaded from the HitBTC application programming interface (<https://api.hitbtc.com>) for  $N = 10^5$  minutes ending on 2019-08-12. Three currencies with insufficient historical data were dropped and a portfolio was formed with  $M = 17$  assets: BTC, ETH, EOS, LTC, BCH, TRX, ETC, XMR, NEO, XEM, IOTA, XLM, DASH, ZEC, ADA, DOGE, and XTZ.

The logarithmic returns for the closing price of these digital coins were calculated as:

$$\begin{aligned} r_{m,n} &= \log(p_{m,n+1}) - \log(p_{m,n}) \\ &\approx \frac{p_{m,n+1}}{p_{m,n}} - 1, \end{aligned} \quad (1)$$

where  $p_{m,n}$  is the  $n^{\text{th}}$  closing price for the  $m^{\text{th}}$  digital asset, with  $n = 1 \dots N$ , and  $m = 1 \dots M$ . We then computed the normalized returns that form a matrix  $\mathbf{L}$  with elements:

$$L_{m,n} = \frac{r_{m,n} - \langle r_m \rangle}{\sqrt{\langle r_m^2 \rangle - \langle r_m \rangle^2}}. \quad (2)$$

For any observable in this work we assign:

$$\langle O_m \rangle = \frac{1}{N} \sum_{n=1}^N O_{m,n}. \quad (3)$$

Eugene Wigner has originally proposed in 1955 that the energy levels of heavy nuclei could be described by the eigenvalues of random matrices. A Wigner matrix is then defined as a square matrix that is symmetric (but in more general cases it can also be Hermitian or symplectic), where their elements  $\{h_{ij} | \forall i \leq j\}$  and  $\{h_{ii}\}$  are identically distributed random variables with finite first and second moments. Following this condition we can obtain the joint distribution of its eigenvalues, and integrating all values except one leads to a semicircle law for the the density eigenvalues [6].

The crypto market, however, is composed of a few major crypto currencies that dominate the marketshare. Moreover, most of the alternate cryptocurrencies are constructed on already existing blockchains, which restricts the size of the matrices that can be analyzed. Specifically in our case, there are only  $M = 17$  assets in the portfolio, which may not produce good statistics. To circumvent this problem, we constructed an ensemble of 1000 correlation matrices with  $N = 100$  continuous minute closing prices generated from the original matrix in a bootstrap approach. These are non-square matrices for which the semi-circle law does not apply since not even the eigenvalues can be calculated. Rather, one can use the Marčenko-Pastur law [7] to analyze/compare the density of eigenvalues of the  $M \times M$  correlation matrices:

$$\mathbf{\Lambda} = \frac{1}{N} \mathbf{L} \mathbf{L}^T, \quad (4)$$

with elements related to Eq. 2:

$$\Lambda_{ij} = \frac{\langle r_i r_j \rangle - \langle r_i \rangle \langle r_j \rangle}{\sqrt{\langle (\Delta r_i)^2 \rangle} \sqrt{\langle (\Delta r_j)^2 \rangle}}. \quad (5)$$

This is known as a matrix from the Wishart ensemble and if the elements of  $L$  are mutually uncorrelated identically distributed standard normal random variables, this law states that the density of eigenvalues is given by:

$$\rho(\lambda) = \frac{N}{2\pi M} \frac{\sqrt{(\lambda - \lambda_{\min})(\lambda - \lambda_{\max})}}{\lambda}, \quad (6)$$

where

$$\lambda_{\max,\min} = \left(1 \pm \sqrt{\frac{N}{M}}\right)^2. \quad (7)$$

Thus, it is possible to verify whether the density of eigenvalues of  $\mathbf{\Lambda}$  follows the law described by Eq. 6. Unlike directly computed by other authors (see for example [8]), we calculate the density of eigenvalues of  $\mathbf{\Lambda}$  using the elegant method of Green's function for two reasons: *i)* Our correlation matrix has low dimensionality. Thus, we would run the risk of using insufficient bins for obtaining a meaningful histogram for the density of eigenvalues, and *ii)* This approach explicits the formalism used in quantum mechanics to treat economic problems found in this new field of Econophysics.

### 3. Main results

We discuss our main findings in this section. Since we deal with results related to different aspects of quantum theory we first explain the theory and then present the corresponding results.

#### 3.1. The concept of Eigenportfolios

Our first result discussed in this paper is the concept Eigenportfolios. In order to present it, we should look for a portfolio  $\mathbf{W}$  of the assets (a column vector) that minimizes its volatility and is normalized such that  $\mathbf{W}^T \mathbf{W} = 1$ . The latter is given by the scalar product:

$$\sigma^2 = \mathbf{W}^T \mathbf{\Lambda} \mathbf{W}. \quad (8)$$

Thus, we can construct a Lagrangian function:

$$F = \mathbf{W}^T \mathbf{\Lambda} \mathbf{W} - \lambda(\mathbf{W}^T \mathbf{W} - 1), \quad (9)$$

where  $\lambda$  is a Lagrange multiplier.

The extremum of this function is given by:

$$\mathbf{\Lambda} \mathbf{W} = \lambda \mathbf{W}. \quad (10)$$

Therefore, the portfolio  $\mathbf{W}$  is on the eigenbasis  $|n\rangle$  of the correlation matrix. Futhermore, the normalized eigenvalues  $\lambda_m / \sum_k \lambda_k$  give the explained volatility of the  $m^{\text{th}}$  portfolio.

It is interesting now to compare the obtained explained volatility with one obtained from the Wishart ensemble and another from matrices whose elements are i.i.d. random variables drawn from the Cauchy distribution:

$$f(x; \gamma) = \frac{1}{\pi\gamma} \left[ \frac{\gamma^2}{x^2 + \gamma^2} \right], \quad (11)$$

where  $\gamma$  is a scale parameter which indicates the half-width at half-maximum of the distribution. This distribution was particularly chosen because it is a pathological distribution with fat tails and undefined second moment.

As Fig. 1 indicates, the largest eigenvalue explains approximately 30 % of the variance. Moreover, the cumulative variance is located between those of Gaussian and Cauchy ensembles.

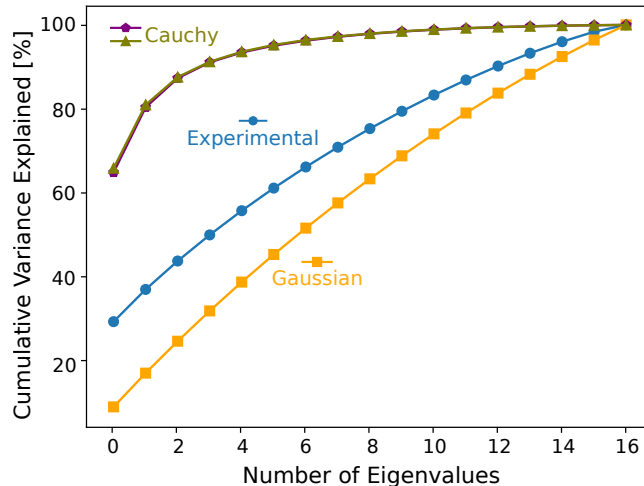


**Figure 1.** Expected cumulative variance explained as a function of the number of eigenvalues for the experimental data, and control series with Gaussian and Cauchy distributions with  $\gamma = 0.1$  (triangle marks) and  $\gamma = 0.45$  (pentagon marks).

We believe that the concept of eigenportfolio deserves further explorations for standard financial assets. Furthermore, it may be used to characterize stylized facts in stock markets. In the next subsection we will present our results corresponding to density of eigenvalues calculated via the Green's function method for the  $M = 17$  assets used in this work. We also compared it with the density obtained for the benchmark distributions.

### 3.2. Density of Eigenvalues via Green's function method

The retarded Green's function associated with the correlation matrix  $\mathbf{\Lambda}$  is given by the resolvent:

$$\mathbf{G}_\eta^R(\lambda) = [(\lambda + i\eta)\mathbf{I} - \mathbf{\Lambda}]^{-1}. \quad (12)$$

It can be written in the eigenbasis of the correlation matrix as:

$$\mathbf{G}_\eta^R(\lambda) = \sum_m |n\rangle \mathbf{C}_m. \quad (13)$$

Combining both equations, we obtain:

$$\mathbf{C}_n = \frac{\langle n |}{(\lambda + i\eta) - \lambda_m}. \quad (14)$$

Therefore, the retarded Green's function can be written as:

$$\mathbf{G}_\eta^R(\lambda) = \sum_\alpha \frac{|n\rangle \langle n|}{\lambda + i\eta - \lambda_m}. \quad (15)$$

Taking the limit where  $\eta \rightarrow 0$ , one obtains:

$$\lim_{\eta \rightarrow 0} \text{Im} \{ \langle n | \mathbf{G}_\eta^R | n \rangle \} = -\pi \delta(\lambda - \lambda_m). \quad (16)$$

Therefore we can calculate the density of states according to:

$$\begin{aligned} \rho(\lambda) &= \frac{1}{M} \sum_{n=1}^M \delta(\lambda - \lambda_m) \\ &= -\frac{\pi}{N} \lim_{\eta \rightarrow 0} \text{Tr} \{ \text{Im} \{ \mathbf{G}_\eta^R(\lambda) \} \}. \end{aligned} \quad (17)$$

Again, we average it over an ensemble of  $n_{\text{sampling}} = 1000$  matrices to get an average density of assets  $\bar{\rho}(\lambda) = \langle \rho(\lambda) \rangle$ .

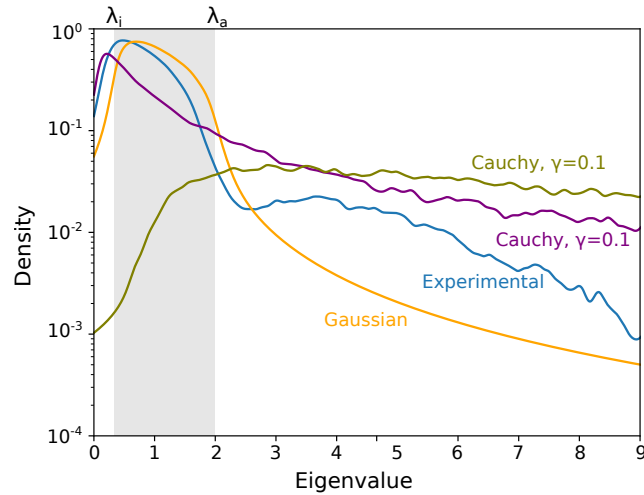


**Figure 2.** Measured density of eigenvalues. The shaded area corresponds to the region between the expected minimum and maximum eigenvalues from the Marčenko-Pastur distribution (Eq. 7). The density of control series with Gaussian and Cauchy distributions are also shown.

Unlike the Gaussian ensemble, the Wishart ensemble does not exhibit level repulsion. Nonetheless, pathological distributions such as the Cauchy with high spacing parameters may show a similar behavior. The density obtained for the series under study in Fig. 2 resembles that of Gaussian ensembles. However, it occupies a region of eigenvalues slightly different than that expected from the Marčenko-Pastur distribution in Eq. 7. The expected theoretical distribution should fit a region between  $\lambda_i = 0.34$  and  $\lambda_a = 1.99$ . However, our data occupies a region between  $\lambda_i = 0.03$  and  $\lambda_a = 11.73$ . Moreover, the tail of the density at large eigenvalues seems to be caused by the tail of the distribution of returns. Having studied the density of eigenvalues and benchmarked it, we will now discuss the quantum localization phenomena applied for cryptocurrencies.

### 3.3. Measures of Localization

Although the portfolio is normalized, its fourth moment is related to the localization of the eigenfunctions and is commonly known as the *inverse participation ratio* [9]:

$$IPR(\lambda_m) = \sum_{k=1}^M |\langle e_k | m \rangle|^4, \quad (18)$$

where  $e_k$  forms a complete orthonormal basis in the Hilbert.

An eigenvector with equal components  $\langle e_k | m \rangle = M^{-1/2}$  has an  $IPR = M^{-1}$ , whereas an eigenvector with only one component different than zero  $\langle e_k | m \rangle = \delta_{mm'}$  has an  $IPR = 1$ . The inverse of  $IPR$ , the participation ratio  $PR$  gives the number of modes in a specific eigenvector. We study the normalized participation ratio, where 1 indicates an *extended state* and  $M^{-1}$  indicates a *localized state*.

This is related to another measure of localization that is given by the Shannon entropy defined as[10]:

$$S(\lambda_m) = - \sum_{k=1}^M |\langle e_k | m \rangle|^2 \log (|\langle e_k | m \rangle|^2). \quad (19)$$

Instead of studying the entropy directly, one can use the *localization length* defined as:

$$\xi(\lambda_m) = \exp (S(\lambda_m)). \quad (20)$$

It is possible to examine the localization length similarly to what is done for the participation ratio. For an extended state  $\langle e_k | M = M^{-1/2}$ , the Shannon entropy gives  $\log(M)$ . Therefore, the normalized localization length gives 1. In the opposite limit, localized states  $\langle e_k | M = \delta_{mm'}$  produce zero entropy, which gives a normalized localization length  $M^{-1}$ .

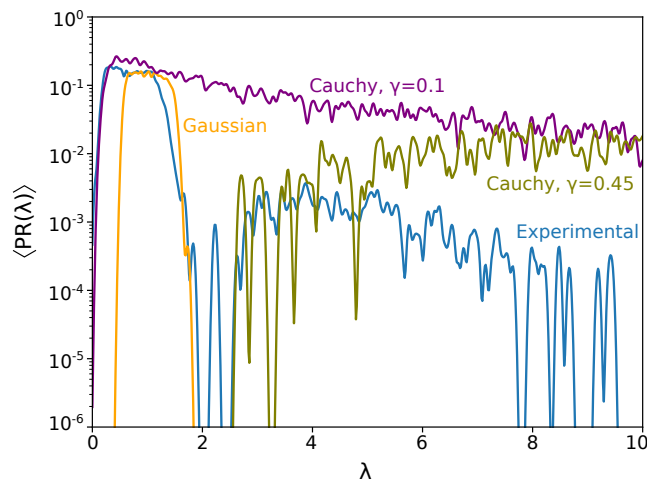


**Figure 3.** Expected participation ratio  $\langle PR(\lambda) \rangle$  obtained for: the time series under study (blue), a Gaussian control (orange), a Cauchy control with scale parameter  $\gamma = 0.1$  (purple), and a Cauchy control with scale parameter  $\gamma = 0.45$  (olive).

In order to obtain an average over the whole time series we adopted the following procedure. First, we construct a function  $\varphi(\lambda)$  with Gaussian functions centered on each eigenvalue:

$$\varphi(\lambda) = \sum_{m=1}^M A_m \exp\left(-\frac{(\lambda - \lambda_m)^2}{2\sigma^2}\right), \quad (21)$$

where  $A_m$  are constants to be determined. Here, from an *ad hoc* point of view, we can consider this function to assume the value of the participation ratio for each eigenvalue:

$$\varphi(\lambda_k) = PR(\lambda_k) = \sum_{m=1}^M A_m \exp\left(-\frac{(\lambda_k - \lambda_m)^2}{2\sigma^2}\right). \quad (22)$$

This produces a set of equations that can be put in a matrix format:

$$\mathbf{EA} = \mathbf{P}, \quad (23)$$

where  $\mathbf{E}$  has elements given by:

$$E_{ab} = \exp\left(-\frac{(\lambda_a - \lambda_b)^2}{2\sigma^2}\right), \quad (24)$$

and  $\mathbf{P}$  has elements given by  $P_a = PR(\lambda_a)$ .

This can be solved to find the coefficients  $A_n$  and construct the function  $\varphi(\lambda)$ . This function is then calculated and averaged for different regions of the time series to produce an expected participation ratio  $\langle PR(\lambda) \rangle$ .

We show the expected participation ratio for the time series under study on Fig. 3. The curve indicates the presence of extended states for small eigenvalues as found for the Wishart ensemble [10]. Nonetheless, this is expected for Gaussian returns in non-square matrices as indicated by our control in the same figure. The presence of a mild localization for higher eigenvalues, on the other hand, is expected for non-square matrices of returns that are non-Gaussian. For instance, we plotted the expected participation ratio for non-square matrices of control returns that follow a Cauchy distribution. As previously reported, the distribution of returns is non-Gaussian and the participation is thus expected to have a non trivial behavior [3]. Our results, though, indicate that the distribution of returns in this study is not as trivial as Gaussian but also not so pathological as Cauchy.

### 3.4. Correlation Structure

The structure of the eigenvectors is typically used to analyze the market. For instance, the market can be divided according to the sign of the elements of the eigenvector corresponding to the largest eigenvalue [11, 8]. The next eigenvectors can then successively be accessed to further cluster the market. We applied this strategy to the assets under study and obtained the tree structure shown in the inset of Fig. 4.

We performed a partition analysis on this tree to study the cluster structure of the market. The links in the tree are progressively cut from left to right and the number of

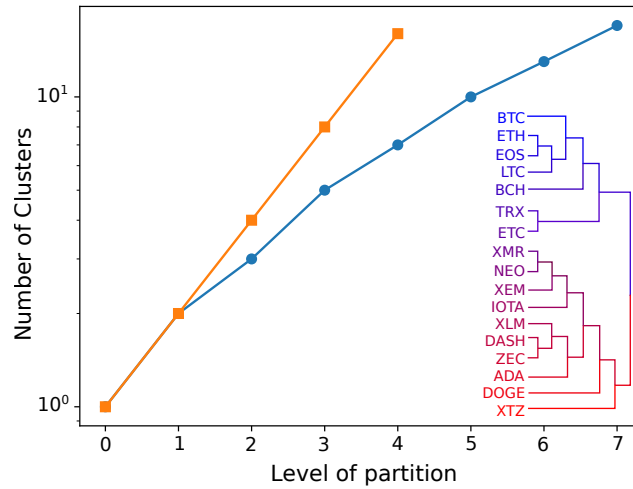


**Figure 4.** Number of clusters as a function of the level of partition for the real data (blue with dots) and for a trivially connected tree (orange with squares). The inset shows a tree diagram for the hierarchical structure of the assets under study.

generated clusters are counted. This result is illustrated in Fig. 4 and compared with the trivial case where a market is uniformly pairwise clustered. The divergence from the trivial case in our results indicates that the assets under study tend to strongly bundle together.

*3.4.1. Networks* We further explore the hierarchical structure of the market by calculating ultrametric spaces, a concept that is borrowed from the theory of frustrated disordered systems[12, 13]. A distance metric between the assets can be described by the Euclidean distance between their return vectors:

$$d_{nm}^E = \|\mathbf{L}_m - \mathbf{L}_n\| = \sqrt{\|\mathbf{L}_m\|^2 + \|\mathbf{L}_n\|^2 - 2\mathbf{L}_m \cdot \mathbf{L}_n} = \sqrt{2(1 - \Lambda_{nm})}. \quad (25)$$

We refer to this metric simply as the Euclidean distance.

Since the structure of the eigenvectors is used to cluster the assets, it is convenient to also use a *spectral distance*. For this, we create vectors whose elements are taken from the same entry of different eigenvectors weighted by the corresponding eigenvalue. The metric is then the Euclidean distance between these vectors:

$$d_{nm}^s = \sqrt{\sum_k \lambda_k^2 [\langle e_n | k \rangle - \langle e_m | k \rangle]^2} \quad (26)$$

We refer to this metric as the spectral distance.

Computing the distances between all assets creates a complete graph. This carries redundant information that can be eliminated if one uses the *minimal spanning tree* (MST) [14, 15]. We construct such backbone of the network choosing links such that the total length of the tree is minimized. We used Prim's algorithm [16] to construct the MST shown in Fig. 5. This algorithm consists of connecting the elements with the smallest distance, then connect the next set of nodes given that no loop is produced,

and repeat this operation until all nodes are connected. Fig. 5 shows the minimum spanning trees constructed with both the Euclidean and the spectral distances.

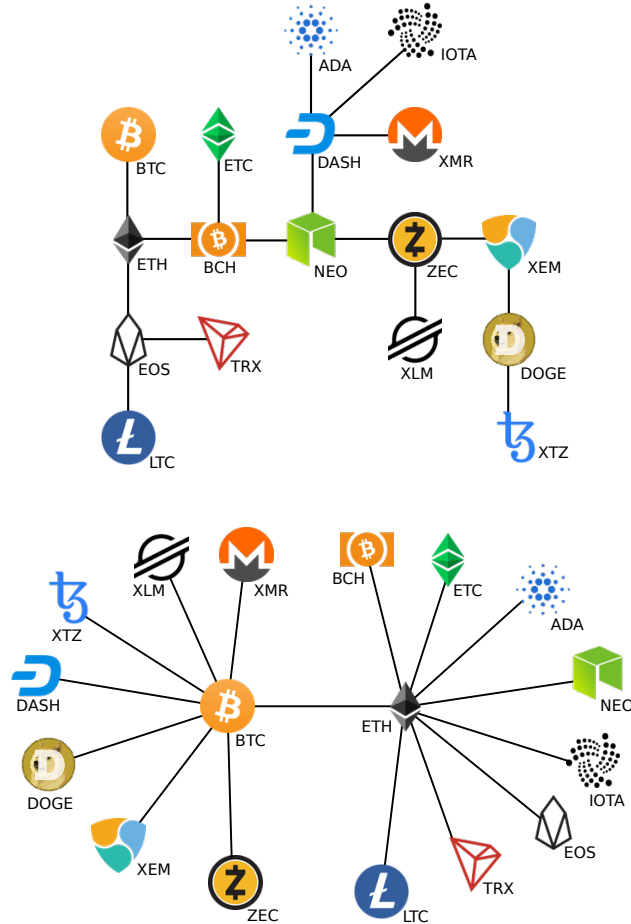


**Figure 5.** Complex network composed using the top) spectral distance, and bottom) Euclidean distance.

The spanning tree created using the spectral distance carries more information than the one created using the Euclidean distance. This happens because the eigenvectors carry information about the relationship between all elements of the correlation matrix, whereas the Euclidean distance is a binary distance between assets. Although the the minimum spanning tree created with the Euclidean distance shows two groups of assets, the one created with the spectral metric is close to the tree created partitioning the assets as shown in Fig. 4. Whereas the former does not say much about the staggering of the assets, the latter shows how the different clusters are formed when the network is partitioned in different manners.

### 3.5. Epps Effect

It is possible to obtain further information about the portfolio studying how the correlations between assets change with the sampling period. We have verified that

both the second moment and the kurtosis of the distribution of returns for bitcoin depends on the sampling period [3]. Also, it has been experimentally observed that the correlation tends to increase with the sampling period [17]. The latter is known as the *Epps effect*.

A theoretical description of the Epps effect can be obtained by considering the orders as obeying a point process [18]. Thus, we write the jump in return for the  $m^{\text{th}}$  asset as:

$$dP^m(t) = \Delta P^m (dM^{m,+}(t) - dM^{m,-}(t)), \quad (27)$$

where  $\Delta P^m$  is the jump size, which we assume to be constant, and  $M^{m,\pm}$  is a counting process that tracks the number of orders that trigger positive and negative changes.

For a Hawkes process [19] given by:

$$d\lambda^{m,p} = \beta(\lambda_\infty - \lambda^{m,p})dt + \alpha \cdot dN^{m,p}, \quad (28)$$

with  $\beta, \lambda_\infty$ , and  $\alpha$  constants, the correlation coefficient is given by:

$$\text{cor}(dP^1, dP^2) = \left( b_0 + \frac{b_1}{\Delta_t} + \frac{b_2}{\Delta_t^2} \right)^{-1/2}, \quad (29)$$

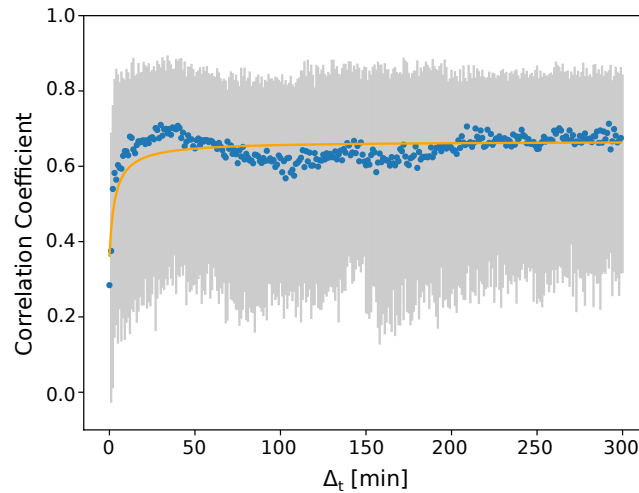
where  $b_0, b_1$ , and  $b_2$  are functions of  $\lambda^{m,p}$ , and  $\Delta_t$  is the sampling period.

Fig. 6 shows the average correlation coefficient obtained for all combinations of assets as well as the minimum and maximum values. The parameters for the average curve are:  $b_0 \approx 2.25$ ,  $b_1 \approx 6.65$ , and  $b_2 \approx -1.41$ . Asynchronicity between orders dominates the average correlation up to a characteristic sampling scale of approximately 20 min. The low-frequency oscillating behavior can be attributed to a time dependency of the estimated parameters which may be caused by the aggregational gaussianity of the assets. Nonetheless, it tends to stabilize after a sampling period of approximately 210 min (3.5 h). Although the trading of cryptographic assets can happen continuously, it is limited by the trading capacity of the exchanges. Thus, the Epps effect found in the correlations between cryptographic assets can, to a large extent, be attributed to the asynchronicity of orders.

#### 4. Discussion and Conclusion

We studied portfolios of 17 digital assets. We computed the correlation matrix for these assets and compared the density of eigenvalues with those of a Wishart ensemble and a non-square matrix of random variables drawn from the Cauchy distribution. Our results indicate that digital assets have a high explained variance but this corresponds to an intermediate behavior between these two control portfolios. Moreover, Wishart ensembles do not show level repulsion as the Wigner matrix. Digital assets show a similar behavior for small eigenvalues, but it approaches the behavior of the Cauchy ensemble for larger eigenvalues.

We developed a new tool based on the superposition of Gaussian functions to perform localization analysis on the eigenvectors of the correlation matrix. Our results



**Figure 6.** Correlation coefficient as a function of the sampling period. Grey lines indicate the maxima and minima whereas the blue circles are the average correlation. The orange line indicates a fitting with the theoretical curve.

indicate that small eigenvalues correspond to highly localized states as is similarly expected for the Wishart ensemble. Furthermore, a mild localization behavior similar to that obtained for the Cauchy ensemble is obtained for larger eigenvalues.

The concept of the minimum spanning tree was also used to investigate the correlation structure of the market of digital assets. We develop a new metric, based on the spectral characteristics of the correlation matrix to explore this behavior and show that the corresponding graph is similar to that obtained by clustering the market according to the elements of its eigenvectors.

## 5. References

- [1] Mantegna R N, Palágyi Z and Stanley H E 1999 *Phys. A* **274** 216–221
- [2] Nakamoto S URL <https://bitcoin.org/bitcoin.pdf>
- [3] da Cunha C R and da Silva R 2019 *arXiv e-prints* arXiv:1905.03211 (*Preprint 1905.03211*)
- [4] Usmani Z, Waddell A and Bieliauskas R 2019 *Invisible Blockchain and Plasticity of Money - Adam Smith Meets Darwin to Buy Crypto Currency (Lecture Notes in Business Information Processing vol 339)* (Springer, Cham) ISBN 978-3-030-04849-5
- [5] Grassberger P 2004 *J. Phys. A: Math. Theor.* **37** 9605
- [6] Wigner E 1958 *Ann. Math.* **67** 325–328
- [7] Marčenko V A and Pastur L A 1967 *Mat. Sv.* **72** 507–536
- [8] Plerou V, Gopikrishnan P, Rosenow B, Nunes L A, Guhr T and Stanley H E 2002 *Phys. Rev. E* **65** 066126
- [9] Guhr T, Müller-Groeling A and Weidenmüller H A 1998 *Phys. Rep.* **299** 189–425
- [10] Åberg S 2013 *J. Phys. A: Math. Theor.* **46** 345101
- [11] Coelho R, Richmond R and Hutzler S 2008 *Adv. Complex Syst.* **11** 655–68
- [12] Rammal R, Toulouse G and Virasoro M A 1986 *Rev. Mod. Phys.* **58** 765–788
- [13] Naylor M J, Rose L C and Moyle B J 2007 *Physica A* **389** 199–208
- [14] Mantegna R N 1999 *Eur. Phys. J. B* **11** 193–196
- [15] Górski A Z, Drożdż S and Kwapien J 2008 *Eur. Phys. J. B* **66** 91–96

- [16] Prim R C 1957 *Bell System Techn. J.* **36** 1389–1401
- [17] Epps T W 1979 *J. Am. Stat. Assoc.* **74** 291–298
- [18] Huth N and Abergel F 2011 *High Frequency Correlation Modelling* (Springer)
- [19] Hawkes A G 1971 *Biometrika* **58** 83–90